Materials Science and Engineering C 33 (2013) 2031–2036

Contents lists available at SciVerse ScienceDirect

Materials Science and Engineering C

journal homepage: www.elsevier.com/locate/msec

ZnS nanoparticles electrodeposited onto ITO electrode as a platform for fabrication of enzyme-based biosensors of glucose

Jian Du, Xiuping Yu, Ying Wu, Junwei Di *

College of Chemistry, Chemical Engineering and Material Science, Key Lab of Health Chemistry and Molecular Diagnosis of Suzhou, Soochow University, Suzhou, Jiangsu 215123, PR China

ARTICLE INFO

Article history:
Received 5 January 2012
Received in revised form 8 December 2012
Accepted 11 January 2013
Available online 17 January 2013

Keywords:
ZnS nanoparticles
Glucose
Electrochemical biosensor
Photoelectrochemical biosensor

ABSTRACT

The electrochemical and photoelectrochemical biosensors based on glucose oxidase (GOD) and ZnS nanoparticles modified indium tin oxide (ITO) electrode were investigated. The ZnS nanoparticles were electrodeposited directly on the surface of ITO electrode. The enzyme was immobilized on ZnS/ITO electrode surface by sol–gel method to fabricate glucose biosensor. GOD could electrocatalyze the reduction of dissolved oxygen, which resulted in a great increase of the reduction peak current. The reduction peak current decreased linearly with the addition of glucose, which could be used for glucose detection. Moreover, ZnS nanoparticles deposited on ITO electrode surface showed good photocurrent response under illumination. A photoelectrochemical biosensor for the detection of glucose was also developed by monitoring the decreases in the cathodic peak photocurrent. The results indicated that ZnS nanoparticles deposited on ITO substrate were a good candidate material for the immobilization of enzyme in glucose biosensor construction.

1. Introduction

In recent decades, Quantum dots (QDs) have attracted worldwide attention and have been extensively studied due to their unique physical and chemical properties [1–3]. For examples, QDs have high photoluminescence quantum efficiency, size-tunable fluorescence emission wavelength and long luminescence lifetimes, which are gradually replacing the conventional organic dyes in various biomedical applications [4–6]. In the luminescent probes and labeling, CdE (E = S, Se, Te) have developed fast and have been commonly used. However, CdE are poisonous and likely to pollute the environment. The inhalation of CdE dust can substantially affect the bone (bone weakness) and kidneys (impairment), and the CdE is carcinogenic to humans [7,8].

ZnS, another semiconductor, is nontoxic to human body, and is very cheap and abundant [7–10]. It is the most suitable candidate to fabricate CdE–ZnS core–shell structures, which could reduce the toxic problems of CdE, and at the same time could maintain CdE's excellent fluorescence properties [11–13]. On the other hand, the ZnS band gap energy is about 3.7 eV, which enables it to be transparent to almost all wavelength of the solar spectrum [14,15]. It appears to be a very promising material for photocatalysis because of the repaid generation of electron–hole pairs by photoexcitation and highly negative reduction potentials of excited electrons [16–19].

Recently, QDs have also been used to immobilize protein for the fabrication of electrochemical biosensors [20,21] and photoelectrochemical biosensors [22,23]. A few papers have reported that the direct electron transfer between enzyme and electrode could be realized using CdE nanoparticles and CdE–ZnS core–shell nanostructures[21,24,25]. It was also reported that ZnS nanoparticles can be used to fabricate a reagentless uric acid biosensor [26]. Moreover, Impellizzeri et al. indicated that ZnS shell seems to dominate the electrochemical properties of CdE–ZnS core–shell nanoparticles, while having a modest effect on their optical properties [13]. Therefore, in QDs, ZnS nanoparticles seem to be more favorable in the application of enzyme based biosensors because of simple preparation, low cost and less toxicity.

In order to fabricate electrochemical biosensors, ZnS nanoparticles must be supported on the solid electrode surface. The use of suitable linker molecules, such as 1-ethyl-3-(3-dimethylaminopropryl) carbodiimide, would be a representative method. The ZnS-modified electrode then immobilized protein to formulate enzyme electrode. However, this method with linker molecules suffers some complexity and disadvantages. It is because they need three steps: i) preparation of ZnS nanoparticles with organic stabilizers, such as Cetyltrimethylammonium (CTA) [27], trioctylphosphine oxide (TOPO) [11,21], sodium bis(2-ethylhexy) sulfosuccinate [28], mercaptoacetic acid [29] and other surfactants [30–32], which may result in relative poor stability and bioactivity of enzyme; ii) surface modification with linker molecules, which may influence its electrocatalytic properties; iii) combination of ZnS nanoparticles with linker molecules. The organic reagents may be toxic and result in a poor contact between the nanoparticles and electrode. Therefore, it is still a challenge to seek simpler method for fabrication of electrochemical biosensor based on ZnS nanoparticles.

The electrodeposition of nanomaterials on the electrode surface is a simple method as well as high surface areas which are solidly attached to the solid substrate. In this paper, ZnS nanoparticles are directly

* Corresponding author. Tel./fax: +86 512 65880089.
E-mail address: djw@suda.edu.cn (J. Di).

0928-4931/$ – see front matter © 2013 Elsevier B.V. All rights reserved.
http://dx.doi.org/10.1016/j.msec.2013.01.019

electrodeposited on the surface of indium tin oxide (ITO) electrode without using any link molecules and organic solvents. The sol–gel (SG) technology was employed to immobilize the glucose oxidase (GOD) on the ZnS film. The direct electron transfer of GOD is realized at the GOD-SG/ZnS/ITO electrode. The obtained biosensor can catalyze the reduction of oxygen and determine the concentration of glucose. The photocatalytic property of ZnS nanoparticles is also investigated and the glucose sensing sensitivity of the biosensor under illumination is higher than that without illumination.

2. Experimental

2.1. Materials

Zinc chloride ($ZnCl_2$) was obtained from Sinopharm Chemical Reagent Co., Ltd. Sodium thiosulphate ($Na_2S_2O_3$) and glucose were purchased from Shanghai Chemical Reagent Company (Shanghai, China). Glucose oxidase (from *Aspergillus niger*, 155,000 Ug^{-1}) was purchased from Sigma Chemical Company. A 1000 U mL^{-1} GOD stock solution was stored at 4 °C. PVA stock solution of 0.25 was prepared by dissolving polyvinyl alcohol (PVA-124, average degree of polymerization was 2400–2500, Shanghai Chemical Reagent Plant imported from Japan). Na_2HPO_4 and NaH_2PO_4 were employed to prepare the 0.02 M phosphate buffer solutions (pH 7.0). Indium tin oxide glass (1.1 mm thickness, less than 100 Ω) was purchased from Suzhou NSG Electronics Co., Ltd. (Suzhou, China). All chemicals were analytical grade and were used as received without further purification. All solutions were made up with twice-distilled deionized water through the study.

2.2. Apparatus

Cyclic voltammetric experiments were performed with a CHI830B electrochemical workstation (Shanghai Chenhua Apparatus Inc., China). A traditional three-electrode configuration was used, with an ITO modified electrode, a platinum wire counter electrode and a saturated calomel reference electrode (SCE) served as working electrode, auxiliary electrode and reference electrode, respectively. All potentials were reported with respect to SCE electrode. The photoelectrochemical measures were performed with a Xenon lamp (350 W) as irradiation source. All the measurements were carried out at a room temperature with the electrolyte which was deoxygenated by purged with nitrogen for at least 10 min prior to experiments, and a nitrogen atmosphere was maintained over the solution during the performance. Scanning electron microscopy (SEM) was run with an S-4700 scanning electron microanalyzer (Hitachi, Japan).

2.3. Fabrication of ZnS/ITO electrode

ZnS/ITO modified electrode was prepared using electrochemical deposition [8,33]. Briefly, a sheet of ITO (0.6 × 3.0 cm) was ultrasonicated with dilute ammonia, absolute ethanol and deionized water for approximately 5 min, respectively. Then, the ITO electrode was immersed in the mixed solution containing 4.0 mL of 2 mM $Na_2S_2O_3$ solution, 4.0 mL of 0.1 M $ZnCl_2$ in a total 10 mL (if necessary add some HCl to adjust pH between 2 to 3) at 50 °C. The electrolysis was carried out in the potential range from −0.4 to −1.0 V at 50 mV/s for 40 cycles in cyclic voltammetry. After deposition, the electrode was removed from the solution and washed with water.

2.4. Synthesis of GOD-SG/ZnS/ITO electrode

The preparation of silica colloidal sol was done according to the previous report [34]. Briefly, $Na_2SiO_3 \cdot 9H_2O$ was stored at 110 °C for 12 h. After cooling down, the resulting solution was adjusted with 3 M HCl to specific gravity of 1.38. Then, the silica sol was fabricated by ion-exchange method from the diluted (addition of same volume water) solution. Dip the ZnS/ITO electrode in the following solution: 0.3 mL of 1000 U/mL GOD, 0.3 mL of silica sol solution, 0.1 mL of 0.25 PVA in each milliliter. Then dry the electrode under nitrogen atmosphere. The enzyme electrode (defined as GOD-SG/ZnS/ITO) was stored at 4 °C in a refrigerator when not in use. For comparison, the SG/ZnS/ITO was prepared by the same method but without addition of GOD and GOD-SG/ITO was fabricated by the same method on ITO electrode. The GOD/ZnS/ITO electrode was fabricated by immersing the ZnS/ITO electrode in GOD solution for 2 h.

3. Results and discussion

3.1. Characteristics of ZnS/ITO modified electrode

ZnS nanoparticles were deposited directly on ITO surface by electrochemical method. Although the exact mechanism of the consecutive electrochemical or electrochemical–chemical steps is still not clear, the cathodic deposition of MS from electrolyte of M^{2+} and $S_2O_3^{2-}$ions was not a doubt [35]. The ZnS/ITO modified electrode was almost colorless. It turned brownish back after addition of a drop of $Pb(NO_3)_2$ solution. This indicates that S element was existent. The composition of Zn was demonstrated by ICP-AES after the nanoparticles were dissolved in acid. The XRD patterns were recorded for the deposited products before and after treated at 500 °C in Fig. 1A. No pronounced ZnS or Zn peak was observed in the product before and after treated at 500 °C in N_2 environment. After treated at 500 °C in air atmosphere, several new small peaks located at 35.8°, 56.1°, and 62.3° were observed, which is attributed to ZnO crystalline of (101), (110), and (103) planes[36]. These results indicate that the crystallinity of ZnS electrodeposited on ITO substrate was very low.

The SEM is also employed to evaluate the physical appearance and surface features of the nanomaterials. The image of bare ITO surface was rather smooth (Fig. 1B). It is observed that ZnS nanoparticles were grown successfully on the ITO surface with quasi-spherical (Fig. 1C). The average diameter of these nanoparticles was around 20 nm. The coverage of the nanoparticles on substrate surface could be controlled by adjusting the potential and electrodeposition cycles. From the scrape in the film, it can clearly be seen that the silica sol–gel film was formed onto the ZnS/ITO surface (Fig. 1D).

3.2. Electrochemical behavior of the GOD-SG/ZnS/ITO electrode

The GOD was immobilized on ZnS/ITO surface by sol–gel technique. Therefore, enzyme was embedded in the silica sol–gel network. Fig. 2 shows the typical cyclic voltammograms at the different modified electrodes in 0.02 M phosphate buffer solution (pH 7.0). There were no obvious redox peaks at the bare ITO and SG/ZnS/ITO electrodes. A very little peak was observed at GOD-SG/ITO electrode. However, a pair of stable and well-defined redox peaks was obtained at the GOD-SG/ZnS/ITO electrode, which was also much higher than that obtained at the GOD/ZnS/ITO electrode. It suggests that ZnS nanoparticles promote the electron transfer between the enzyme embedded in silica sol–gel network and electrode without the help of mediators. The formal potential (E^0) was −0.45 V with a small peak potential separation (ΔEp) of 30 mV. This value was smaller than that of 94 mV at GOD/Au modified electrode [37], 78 mV at GOD/carbon ionic liquid electrode (CILE) modified electrode [38], 56 mV at GOD/$NdPO_4$ NPs/Chitosan modified electrode [39] and 35 mV at GOD/SnO_2-Au/modified electrode [40]. This demonstrates that ZnS nanoparticles are favorable in the preparation of enzyme-based electrochemical biosensors.

Fig. 3 shows the CVs of the GOD-SG/ZnS/ITO electrode at different scan rates in 0.02 M phosphate buffer solution (pH 7.0). The peak-to-peak separation increased gradually with the increase of scan rate. The oxidation peak shifted to more positive potentials and the reduction peak shifted to more negative potentials. Both the anodic and

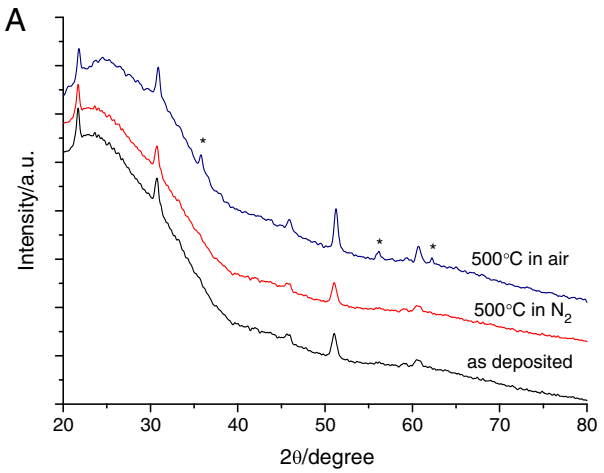

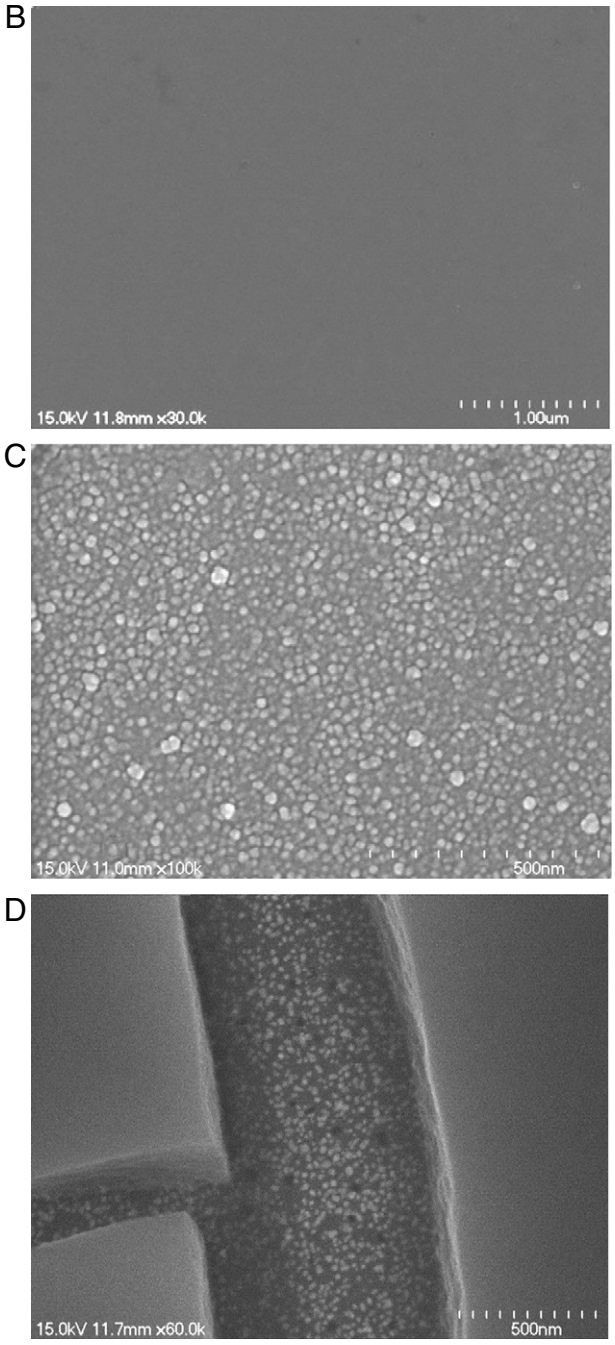

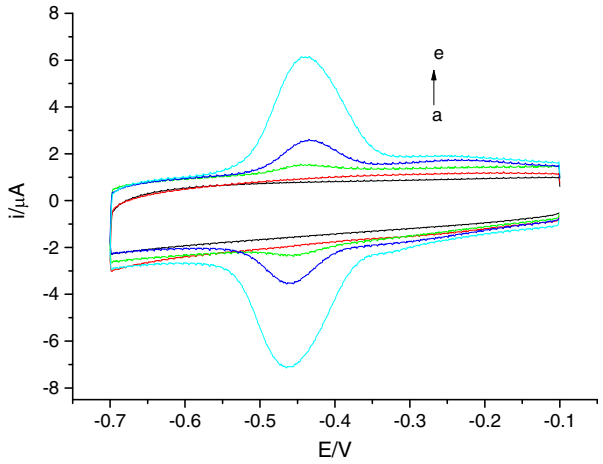

Fig. 2. Cyclic voltammograms at the bare ITO (a), ZnS/ITO (b), GOD-SG/ITO (c), GOD/ZnS/ITO (d), and GOD-SG/ZnS/ITO (e) electrodes in 0.02 M phosphate buffer solution (pH 7.0). Scan rate: 100 mV/s.

cathodic peak currents increased linearly with the potential scan rate (inset of Fig. 3), which indicates a typical surface-controlled process [20,41]. In order to obtain the kinetic parameter of GOD redox, the scan rate was increased. It was found that when scan rate was above 1.0 V/s, the difference of anodic and cathodic peak potentials was more than 0.2 V. The anodic and cathodic peak potentials are proportional to the logarithm of the scan rates with slopes of $2.3RT/(1-\alpha)nF$ and $-2.3RT/\alpha nF$ at high scan rate. From the slope, the electron transfer coefficient (α) was calculated to be 0.54. The electron transfer rate constant k_s of the GOD was evaluated to be 5.7 s^{-1} according to the Laviron equation [42,43]. The value was close to those of 5.0 s^{-1} at GOD/SnO_2-Au/modified electrode [40], 2.5 s^{-1} at GOD/carbon-coated nickel modified electrode [41], 3.8 s^{-1} at GOD/CdS-CNT modified electrode [44] and 3.98 s^{-1} at GOD/CILE-nafion modified electrode [38]. It further demonstrated that the ZnS nanoparticles provide a good microenvironment for GOD to realize direct electron transfer between enzyme and electrode.

Cyclic voltammogram at GOD-SG/ZnS/ITO electrode had a strong relationship with the solution pH. As shown in Fig. 4, both the anodic and cathodic peak potentials shifted negatively with increasing the solution pH from 5.8 to 8.0. The formal potential of GOD-SG/ZnS/ITO decreased linearly with the increase of pH value. The slope was about −56 mV/pH, which was much closer to the theoretical value of −58 mV/pH. It implied that the same protons and electrons were involved in the electron transfer process. The peak currents arrived at the maximum at pH 7.0. Therefore, all the subsequent experiments followed in the pH 7.0 buffer solution.

3.3. Optimization of the ZnS nanoparticles deposition

The electrodeposition voltage plays an important role in the performance of the enzyme electrode. The applied potential range was investigated, while the positive voltage was fixed at −0.4 V. Fig. 5A shows the relationship between the cathodic peak current of the enzyme electrode and the potential in ZnS deposition. The maximum cathodic peak current appeared in the range of −0.4 to −1.0 V. For more negative applied potential, the cathodic peak current decreased rapidly due to serious aggregation of ZnS nanoparticles. This aggregation is attributed to the deposition of more number of ZnS nanoparticles and the growth of larger size of particles. Therefore, the electrodeposition voltage was set from −0.4 V to −1.0 V.

Fig. 1. XRD patterns of deposited ZnS nanomaterials before and after treated at 500 °C in N_2 and air atmosphere A), and SEM image of bare ITO (B), ZnS/ITO (C), and GOD-SG/ZnS/ITO (D).

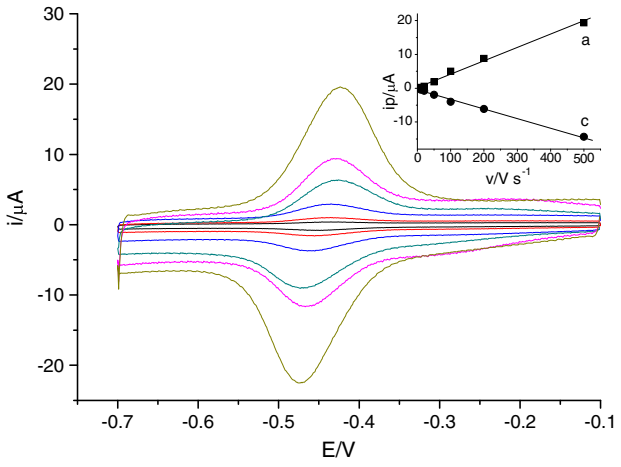

Fig. 3. Cyclic voltammograms of GOD-SG/ZnS/ITO in 0.02 M phosphate buffer solution (pH 7.0) solution at various scan rates of (from inner to outer) 10, 20, 50, 100, 200 and 500 mV/s. Insert: Relationship between the peak currents and scan rates.

The effect of ZnS electrodeposition cycles on the electrode response was also tested between 5 to 90 cycles (Fig. 5B). The cathodic peak current increased with the increasing electrodeposition from 5 to 40 cycles and then arrived at the plateau more than 40 cycles. Therefore, 40 cycles were recommended and used in the following experiments.

3.4. Electrocatalytical ability of the enzyme electrode

According to the previous report, if the immobilized GOD retained good native structure and catalytic activity, it had good electrocatalytic activity for O_2[20]. No peak was observed at the ZnS/ITO electrode in the presence of dissolved O_2. In the presence of oxygen, the shape of voltammograms of GOD-SG/ZnS/ITO electrode exhibited a significant change with an increase of reduction peak current and decrease of oxidation peak current compared to curve a (Fig. 6). The electrocatalytical mechanism for the GOD can be explained as equations [45]:

$$\mathrm{GOD-FAD} + 2\mathrm{H}^+ + 2\mathrm{e}^- \leftrightarrow \mathrm{GOD-FADH_2} \quad (1)$$

$$\mathrm{GOD-FADH_2} + \mathrm{O_2} \rightarrow \mathrm{GOD-FAD} + \mathrm{H_2O_2} \quad (2)$$

$$\mathrm{GOD-FAD} + \mathrm{glucose} \rightarrow \mathrm{GOD-FADH_2} + \mathrm{gluconolactone}. \quad (3)$$

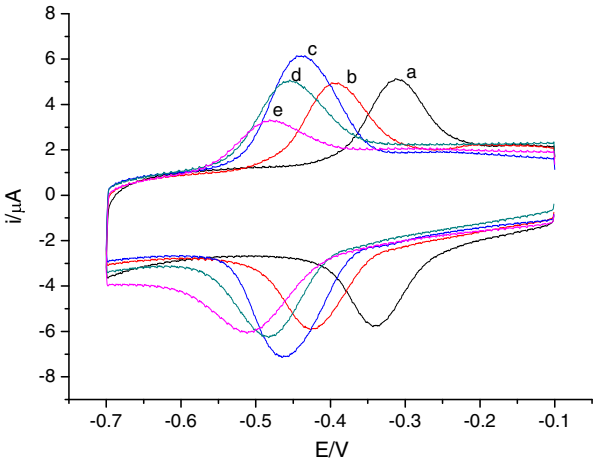

Fig. 4. Cyclic voltammograms at GOD-SG/ZnS/ITO electrode in different pH buffer solutions: a—5.8, b—6.3, c—7.0, d—7.5, and e—8.0. Scan rate: 100 mV/s.

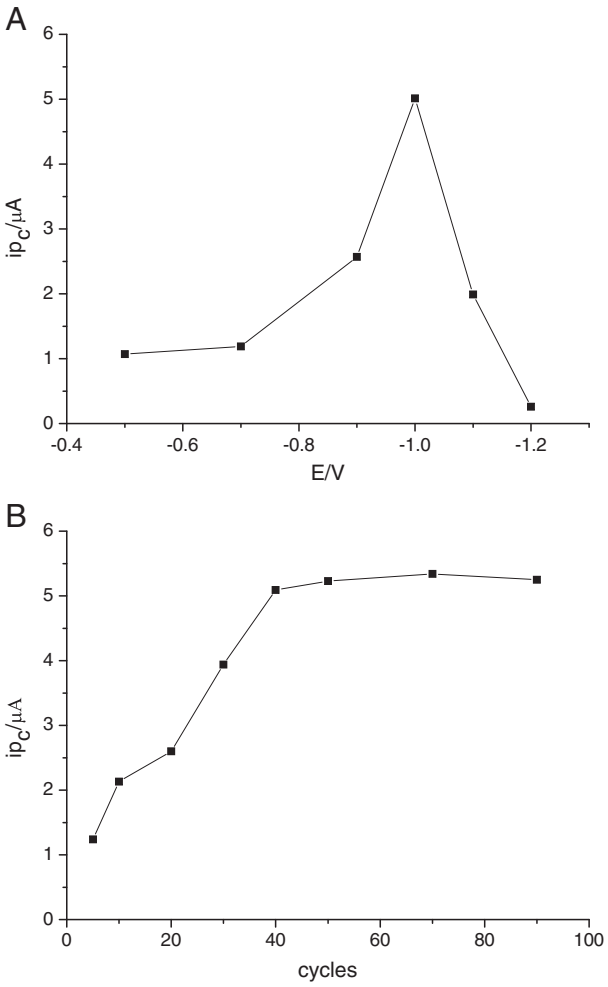

Fig. 5. Dependence of cathodic peak current at GOD-SG/ZnS/ITO electrode on the applied negative potential (A) and electrodeposition cycles (B) in the ZnS deposition.

The absorbed GOD catalyzed the reduction of O_2, which led the reduction peak current to increase dramatically. It demonstrates that the GOD preserves its bioactivity after the immobilization process and also proves that ZnS nanoparticles are suitable for the immobilization of GOD. Furthermore, the reduction current of GOD-SG/ZnS/ITO decreased with the addition of glucose to the air-saturated phosphate

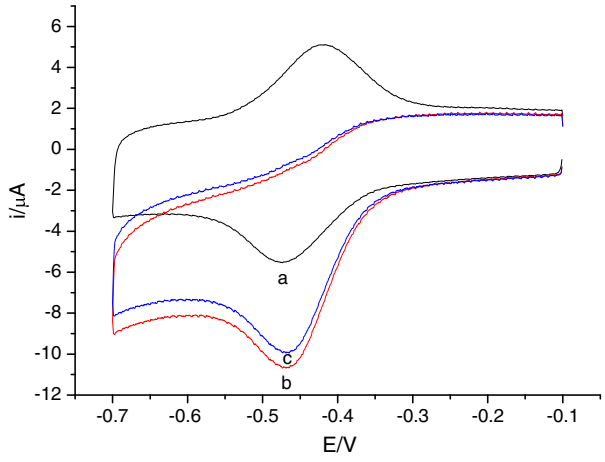

Fig. 6. Cyclic voltammograms of GOD-SG/ZnS/ITO in N_2-saturated buffer solution (a), air-saturated buffer solution (b), and air-saturated buffer solution after addition of glucose (c). Scan rate: 100 mV s^{-1}.

buffer solution (curve c in Fig. 6). Generally, glucose is the substrate of GOD, whose presence will cause the enzyme-catalyzed reaction. It will decrease the oxidized form of GOD on electrode. In other words, the added glucose restrained the electrocatalytic reaction and lead to the decrease of the reduction current, which could be used to determine the glucose concentration [20]. The linear regression equation is $\Delta Ip(\mu A) = 0.095 + 0.549C_{glucose}$ (mM) (r = 0.999) in the glucose concentration range from 0.2 to 5.5 mM. The detection limit was estimated at about 0.04 mM (S/N = 3), which was a little lower than 0.05 mM of GOD based on CdS electrode [24]. The apparent Michaelis–Menten constant (k_m) was equal to 3.8 mM, which was smaller than 5.1 mM for GOD immobilized on CdS. These results further showed that the GOD immobilized on ZnS nanoparticles maintains its bioactivity. ZnS nanoparticles could achieve the equal function of CdS. Therefore, ZnS nanoparticles can replace the toxic CdE to fabricate electrochemical biosensors.

3.5. Photoelectrochemical catalytical ability of the enzyme electrode

QDs exhibited photoelectrochemical activity for its application in amperometric biosensors [46,47]. The photoexcitation of QDs yields electron–hole pairs in the conduction-band and the valence-band under illumination. The valence-band hole can accept the electrons form the substrate while the conduction-band electrons eject to the electrode. The photo electron effect could enhance the charge transfer of redox processes [48]. Therefore, the photoelectrochemical properties of ZnS nanoparticles were also investigated.

Fig. 7 shows the photo-activity of ZnS/ITO in the presence of illumination and absence of illumination. The photocurrent increased dramatically upon illumination and then immediately returned back to its original position when the light was off. As to the control experiment, no photocurrent was observed without the ZnS nanoparticles under illumination. The results indicate that the photocurrent originates from ZnS nanoparticles.

The photoelectrochemical measurements were the same to the voltammograms except for introduction of the irradiation source. The illumination was performed with a Xenon lamp as irradiation source. The enzyme electrode was exposed on the light. The switch was used to control light-on and off conditions. The cathodic peak current in O_2-saturated phosphate buffer solution increased a little with illumination than without illumination. Moreover, the cathodic peak current also decreased linearly with the addition of glucose. The current response under illumination was 1.3 times as much as that without illumination after addition of the same amount of glucose (Fig. 8). Under light on, the linear range for the determination of glucose was 0.1–5.5 mM. The detection limit was 0.02 mM. The mechanism of photoelectrochemical sensing of glucose at GOD-SG/ZnS/ITO electrode is not very clear. A preliminary explanation can be addressed as follows [48]: When ZnS nanoparticles were illuminated, the electron and hole were generated, respectively in the conduction and valence bands. The H_2O_2, produced by the reaction of glucose and O_2 in the presence of GOD, is oxidized by the valence-band hole of ZnS nanoparticles. Meanwhile, the conductive band electron is transferred to the electrode, thus generating a photocurrent. The current response under illumination was the sum of electrochemical current and photocurrent. So the biosensor exhibited higher sensitivity and lower detection limit towards glucose with illumination than without illumination.

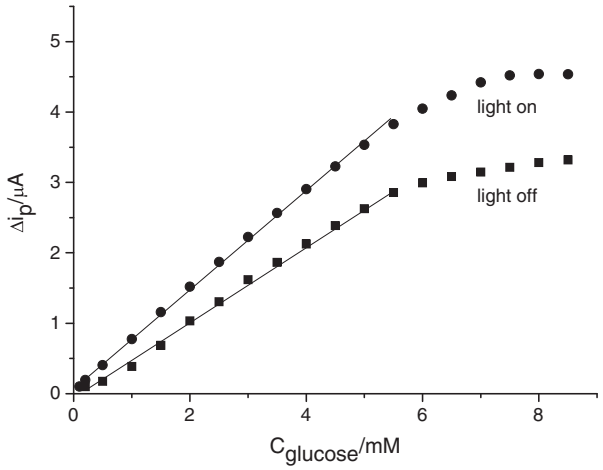

Fig. 8. Calibration of GOD-SG/ZnS NPs/ITO electrode with concentration of glucose upon light on and light off (conditions are the same as those in Fig. 6).

The repeatability of GOD-SG/ZnS/ITO electrode was examined. The relative standard deviation (RSD) of the biosensor response to 0.5 mM glucose was 5.9% for 7 successive measures (Fig. 9). The stability of the GOD-SG/ZnS/ITO enzyme electrode was also studied by comparing the cyclic voltammetric peak currents after successive scan for 30 cycles. The results show almost no decrease of the voltammetric

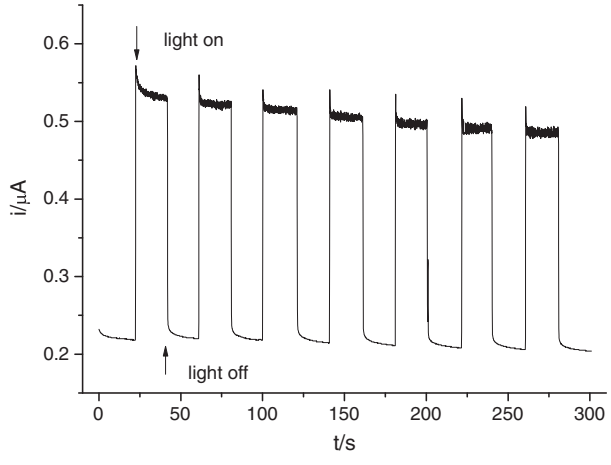

Fig. 7. Photocurrent response of the ZnS/ITO electrode in pH 7.0 phosphate buffer solution. Applied potential: 0.2 V.

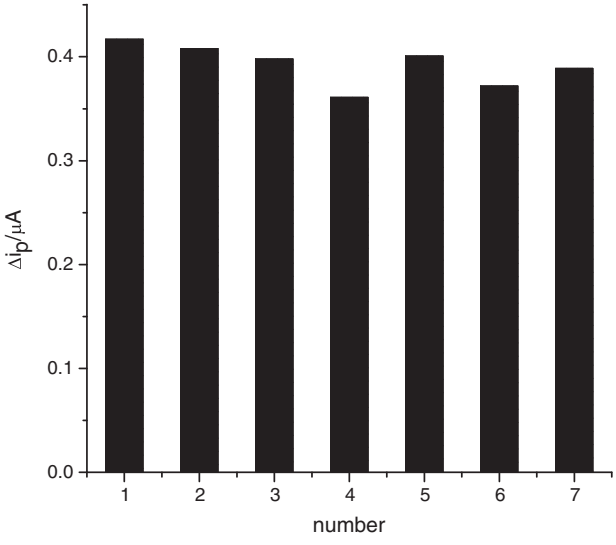

Fig. 9. The repeatability of the biosensors for determination of 0.5 mM glucose.

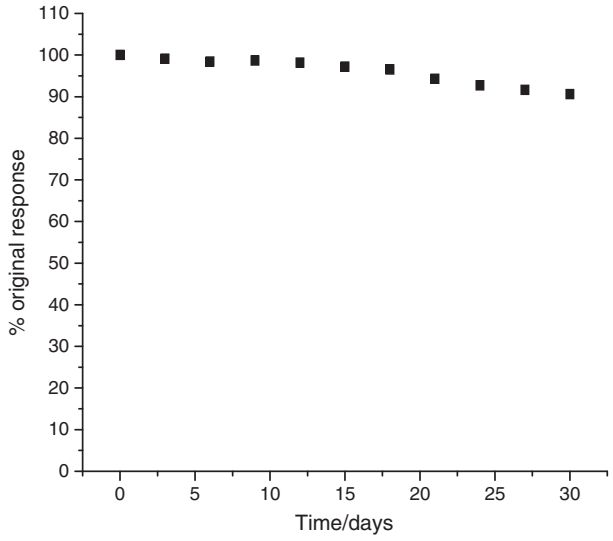

Fig. 10. The multiple use of stability of the biosensor.

current response. The storage stability of this biosensor was investigated by repetitive measurements during 1 month. The sensor was stored in the dry state at 4 °C between measurements. The sensor retained more than 90% of its initial response to the oxidation of glucose (Fig. 10). It indicates the stable property of the enzyme electrode in the buffer solution. The good stability of the GOD-SG/ZnS/ITO electrode is attributed to the excellent biocompatibility of the ZnS nanoparticles. Moreover, the determination of glucose in serum sample was carried out at the biosensor using standard addition method. The glucose level was measured to be 6.04 mM, close to the value of 6.15 mM obtained by spectrophotometry in the hospital. The recoveries for the assay were between 96.7 and 102.9%. Therefore, the ZnS nanoparticles are efficient for retaining the activity of GOD and can be served as a platform to fabricate electrochemical biosensors and photoelectrochemical biosensors.

4. Conclusions

In summary, ZnS nanoparticles are electrodeposited directly on ITO substrate surface without any organic molecules. Such ZnS nanomaterials with large surface area are favorable to immobilize enzyme in the silica sol–gel network. The direct electron transfer of GOD immobilized on the modified electrode is obtained, which could be used to develop electrochemical and photoelectrochemical biosensors. The approach method provides an efficient strategy and another platform for developing a variety of bioelectrochemical and photoelectrochemical devices.

Acknowledgment

The authors would like to thank the National Natural Science Foundation of China (no. 21075086), the Project of Scientific and Technologic Infrastructure of Suzhou (SZS201207) and the Priority Academic Program Development of Jiangsu Higher Education Institutions are gratefully acknowledged.

References

[1] H.M.E. Azzazy, M.M.H. Mansour, S.C. Kazmierczak, Clin. Biochem. 40 (2007) 917–927.
[2] Y. Zhang, H. Zhang, X. Guo, H. Wang, Microchem. J. 89 (2008) 142–147.
[3] D.P. Halliday, J.M. Eggleston, K. Durose, Thin Solid Films 322 (1998) 314–318.
[4] X. Feng, Q. Shang, H. Liu, W. Wang, Z. Wang, J. Liu, J. Lumin. 130 (2010) 648–653.
[5] W.J. Jin, J.M. Costa-Fernández, R. Pereiro, A. Sanz-Medel, Anal. Chim. Acta 522 (2004) 1–8.
[6] C.P. Huang, S.W. Liu, T.M. Chen, Y.K. Li, Sensors Actuators B 130 (2008) 338–342.
[7] T. Miyawaki, M. Ichimura, Mater. Lett. 61 (2007) 4683–4686.
[8] N. Fathv, M. Ichimura, Sol. Energy Mater. Sol. Cells 87 (2005) 747–756.
[9] S.W. Shin, S.R. Kang, J.H. Yun, A.V. Moholkar, J.H. Moon, J.Y. Lee, J.H. Kim, Sol. Energy Mater. Sol. Cells 95 (2011) 856–863.
[10] S.K. Mehta, Khushboo, A. Umar, Talanta 85 (2011) 2411–2416.
[11] X. Fu, K. Huang, S. Liu, J. Microbiol. Methods 79 (2009) 367–370.
[12] H.D. Duong, J.I. Rhee, Talanta 73 (2007) 899–905.
[13] S. Impellizzeri, S. Monaco, I. Yildiz, M. Amelia, A. Credi, F.M. Raymo, J. Phys. Chem. C 114 (2010) 7007–7013.
[14] X. Fang, T. Zhai, U.K. Gautam, L. Li, L. Wu, Y. Bando, D. Golberg, Prog. Mater. Sci. 56 (2011) 175–287.
[15] L. Qi, G. Mao, J. Ao, Appl. Surf. Sci. 254 (2008) 5711–5714.
[16] Y. Ni, X. Cao, G. Hu, Z. Yang, X. Wei, Y. Chen, J. Xu, Cryst. Growth Des. 7 (2007) 280–285.
[17] P.P. Hankare, P.A. Chate, D.J. Sathe, J. Alloys Compd. 487 (2009) 367–369.
[18] Y. Xie, C. Zhang, S. Miao, Z. Liu, K. Ding, Z. Miao, G. An, Z. Yang, J. Colloid Interface Sci. 318 (2008) 110–115.
[19] C. Wang, Y. Ao, P. Wang, S. Zhang, J. Qian, J. Hou, Appl. Surf. Sci. 256 (2010) 4125–4128.
[20] Q. Liu, X. Lu, J. Li, X. Yao, J. Li, Biosens. Bioelectron. 22 (2007) 3203–3209.
[21] Z. Wang, Q. Xu, H.Q. Wang, Q. Yang, J.H. Yu, Y.D. Zhao, Sensors Actuators B 138 (2009) 278–282.
[22] L. Tang, Y. Zhu, X. Yang, J. Sun, C. Li, Biosens. Bioelectron. 24 (2008) 319–323.
[23] Y. Huang, W. Zhang, H. Xiao, G. Li, Biosens. Bioelectron. 21 (2005) 817–821.
[24] M. Zheng, Y. Cui, X. Li, S. Liu, Z. Tang, J. Electroanal. Chem. 656 (2011) 167–173.
[25] J. Qian, S. Yan, Z. Xiao, J. Colloid Interface Sci. 366 (2012) 130–134.
[26] F. Zhang, C. Li, X. Li, X. Wang, Q. Wan, Y. Xian, L. Jin, K. Yamamoto, Talanta 68 (2006) 1353–1358.
[27] O. Kozák, P. Praus, K. Koči, M. Klementová, J. Colloid Interface Sci. 352 (2010) 244–251.
[28] J. Zhang, M. Xiao, Z. Liu, B. Han, T. Jiang, J. He, G. Yang, J. Colloid Interface Sci. 273 (2004) 160–164.
[29] L. Li, R. Bian, Y. Ding, M. Yu, D. Yu, Mater. Chem. Phys. 113 (2009) 905–908.
[30] P.S. Khiew, S. Radiman, N.M. Huang, M.S. Ahmad, K. Nadarajah, Mater. Lett. 59 (2005) 989–993.
[31] S.K. Mehta, S. Kumar, Mater. Chem. Phys. 131 (2011) 94–101.
[32] Y. Zhang, X. Liang, L. Li, Mater. Lett. 64 (2010) 1521–1523.
[33] N. Fathy, R. Kobayashi, M. Ichimura, Mater. Sci. Eng. B 107 (2004) 271–276.
[34] J. Wang, L. Wang, J. Di, Y. Tu, Sensors Actuators B 135 (2008) 283–288.
[35] K. Zarębska, M. Skompska, Electrochim. Acta 56 (2011) 5731–5739.
[36] D. Raoufi, Renew. Energy 50 (2013) 932–937.
[37] S. Liu, H. Ju, Biosens. Bioelectron. 19 (2003) 177–183.
[38] L. Liu, Y. Cheng, F. Sun, J. Yang, Y. Wu, J. Solid State Electrochem. 16 (2012) 1003–1009.
[39] Q. Sheng, K. Luo, L. Li, J. Zheng, Bioelectrochemistry 74 (2009) 246–253.
[40] F. Li, J. Song, F. Li, X. Wang, Q. Zhang, D. Han, A. Ivaska, L. Niu, Biosens. Bioelectron. 25 (2009) 883–888.
[41] E. Laviron, J. Electroanal. Chem. 101 (1979) 19–28.
[42] L. Yang, H. Xiong, X. Zhang, S. Wang, X. Zhang, Biosens. Bioelectron. 26 (2011) 3801–3805.
[43] X. Kang, J. Wang, H. Wu, I.A. Aksay, J. Liu, Y. Lin, Biosens. Bioelectron. 25 (2009) 901–905.
[44] J. Yang, R. Zhang, Y. Xu, P. He, Y. Fang, Electrochem. Commun. 10 (2008) 1889–1892.
[45] R. Garjonyte, A. Malinauskas, Biosens. Bioelectron. 15 (2000) 445–451.
[46] X. Zhang, S. Li, X. Jin, X. Li, Biosens. Bioelectron. 26 (2011) 3674–3678.
[47] X. Ren, D. Chen, X. Meng, F. Tang, X. Hou, D. Han, L. Zhang, J. Colloid Interface Sci. 334 (2009) 183–187.
[48] J. Sun, Y. Zhu, X. Yang, C. Li, Particuology 7 (2009) 347–352.